



# Modeling and simulation of solar flat plate collector for energy recovery at varying regional coordinates

Imran Nazir Unar<sup>1</sup> · Ghulamullah Maitlo<sup>2</sup> · Sikandar Ali Abbasi<sup>3</sup> · Masroor Abro<sup>1</sup> · Raja Fahad Qureshi<sup>1</sup> · Sheeraz Ahmed Memon<sup>4</sup> · Tanveer Hussain<sup>5</sup> · Kashif Hussain Mangi<sup>6</sup>

Received: 27 March 2021 / Accepted: 4 August 2021 / Published online: 19 August 2021

© The Author(s), under exclusive licence to Springer-Verlag GmbH Germany, part of Springer Nature 2021

## Abstract

Pakistan has remained an energy-deficient country, and most of the industrial sectors are closed due to the loading shedding of electricity. Even though Pakistan is located on the “solar belt” and receives over 2 MWh/m<sup>2</sup> solar irradiation per year with 1500–3000 h of sunshine, unfortunately solar energy is not harnessed to fulfill the energy needs of the country. Solar flat plate collectors (SFPC) are widely employed for collecting solar radiations from the sun. Currently, worldwide solar thermal energy is widely used in household and commercial equipment for energy collection and utilization. The working fluid selected for this research work is water; numerical simulations were performed using Ansys FLUENT. On selected geographical coordinates, solar ray tracing model was employed to incorporate solar heat flux. Nawabshah (NWB), Hyderabad (HYB), Jacobabad (JCB), and Mirpurkhas (MPK) cities were selected for the measuring of performance of SFPC. Firstly, parallel to ground (at a 0° tilt angle) orientation of SFPC was performed. Furthermore, the performance of SFPC was measured using tilt angles of 15°, 30°, and 45°, respectively. The maximum exit water temperature in JCB at a tilt angle of 30° was 97.8 °C in March and a minimum of 88.09 °C in June. In HYD, at a tilt angle of 45°, the maximum temperature rise was recorded at 98.01 °C in November and the minimum was noticed at 76.37 °C in June. While in JCA, at an angle of 30°, the highest temperature was recorded at 97.83 °C in February and a minimum of 78.54 °C in June. The specific aim of this research study was to measure the performance of the SFPC at different tilt angles and at varying geographical coordinates through numerical simulations.

**Keywords** SFPC · CFD · Water · Tilt angle · Performance

## Introduction

Solar flat plate collectors are frequently utilized throughout the world for heating and electricity generation determinations (Akram et al. 2020; Olczak et al. 2020). Solar radiations are employed through solar collectors for the heating of working fluids such as air and water (Jin et al. 2020; Sarafraz et al. 2019; Zaim et al. 2020). Moreover, the heated working fluid taken from the solar collector is employed for commercial and residential purposes including cooking and space heating and that may be directed to the thermal energy storage tanks (Alva et al. 2018; France et al. 2019). The thermal energy storage tanks are used for the application of thermal energy over extended hours (Choudhury and Baruah 2017; Rockenbaugh et al. 2016). Different kinds of solar collectors are available in the markets such as evacuated tube solar collectors, flat plate solar collectors, and parabolic trough collectors (Fathabadi 2020; Zou et al. 2016). Among a wide variety of solar collectors, the solar flat plate collector is most commonly

Responsible Editor: Philippe Garrigues

✉ Ghulamullah Maitlo  
ghulam.maitlo@duet.edu.pk

<sup>1</sup> Department of Chemical Engineering, Mehran University of Engineering and Technology, Jamshoro, Sindh, Pakistan

<sup>2</sup> Department of Chemical Engineering, Dawood University of Engineering and Technology, Karachi, Sindh, Pakistan

<sup>3</sup> Department of Energy and Environmental Engineering, Dawood University of Engineering and Technology, Karachi, Sindh, Pakistan

<sup>4</sup> Institute of Environmental Engineering & Management, Mehran University of Engineering & Technology, Jamshoro, Sindh, Pakistan

<sup>5</sup> Department of Mechanical Engineering, Mehran University of Engineering and Technology, Jamshoro, Sindh, Pakistan

<sup>6</sup> Department of Chemical Engineering, Quaid e Awam University of Engineering Science and Technology, Nawabshah, Sindh, Pakistan

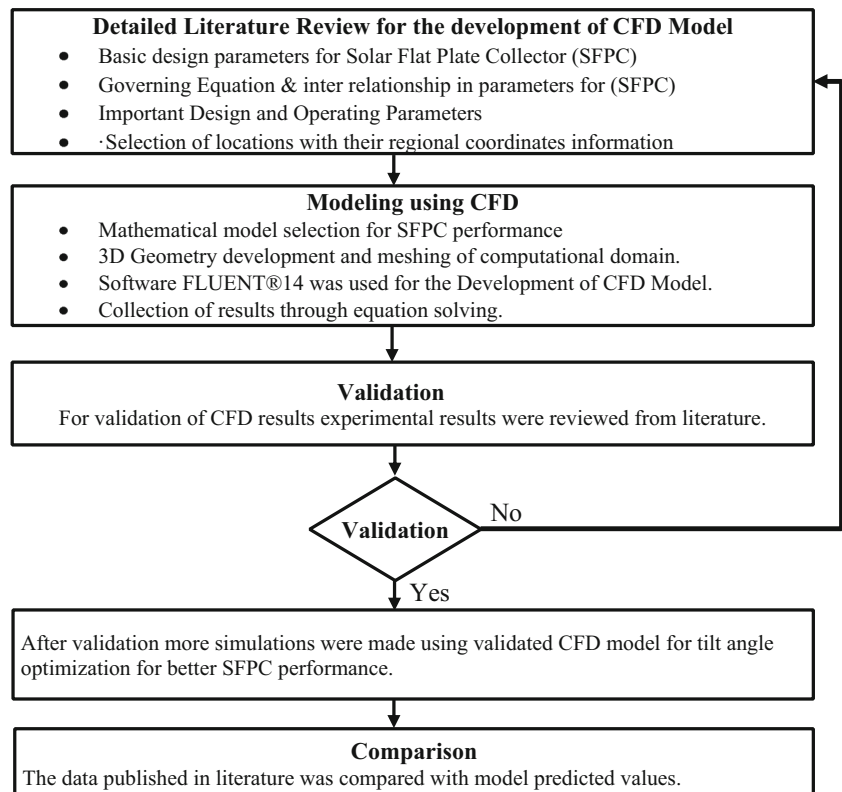
used for domestic and commercial heating applications because of its simplest configurations (Fudholi and Sopian 2019). Furthermore, solar flat plate collectors are extensively investigated keeping in view domestic and industrial water heating systems and for other numerous low-temperature thermal applications (Tiwari et al. 2017). Normally, solar flat plate collectors can supply heat up to a maximum temperature of 90 °C and the mean temperature of ~ 70 °C (Syed et al. 2005). Therefore, solar flat plate collectors emerge as an appropriate choice for residential and commercial buildings as excessive hot water is required in such buildings for laundry washing (Allouhi et al. 2017; Ramlow and Nusz 2010).

Commonly, solar flat plate collectors (SFPC) consists of a shallow metal box covered by a plastic sheet or glass typically known as glazing at the top of the large shallow metal box, while there is a black painted or etched absorber plate at the bottom of the shallow metal box. Furthermore, to avoid heat loss, the sides of the metal box and the bottom surfaces of the collectors are insulated to reduce heat loss to the ambient atmosphere (Kolb et al. 1999; Pottler et al. 1999). The inherent advantages associated with the use of flat collectors are enormous. The manufacturing process of SFPC is easy as compared with other solar thermal equipment. The cost of manufacturing is lower as compared to evacuated tube design. The solar flat plate collector can collect diffuse and direct solar radiations. No complicated tracking equipment and positioning of the solar collector are required. The maintenance of the solar collector is less and easy

(Chabane et al. 2014). The tubes of solar flat plate collectors carrying working fluid and having a circular cross section are numerically and extensively investigated (Khosravi et al. 2019). Besides that, ducts with rectangular cross sections are also extensively investigated for their efficiency. Predominantly, in solar air heaters, rectangular ducts are commonly used (Nahar 2003; Peng et al. 2010). Furthermore, the commercially viable solar collector can cope with ultraviolet radiation, pressure, temperature, and corrosion effects efficiently (Byrne et al. 2011).

Efforts are being done to further reduce cost and increase the durability and thermal efficiency of SFPC (Manikandan et al. 2019). The cost incurred on the purchasing of aluminum and mild steel is less as compared with the purchasing cost of copper, but aluminum and mild steel possess less thermal conductivities when compared with the thermal conductivity of copper. Moreover, mild steel and aluminum tend to corrode during prolonged exposure to ordinary tap water. With the increase in area, the amount of heat transfer to the working fluid increases. The most common problem faced during the increase in absorber duct area results in pressure drop across the collector. The pressure drop requires higher pumping power to pass the working fluid through the collector (Akpınar and Koçyiğit 2010). Therefore, it is significant to set proper dimensions of the solar collector ducts to obtain reasonable economic burden and energy-efficient performance of the collector.

**Fig. 1** The main steps were followed during the research study

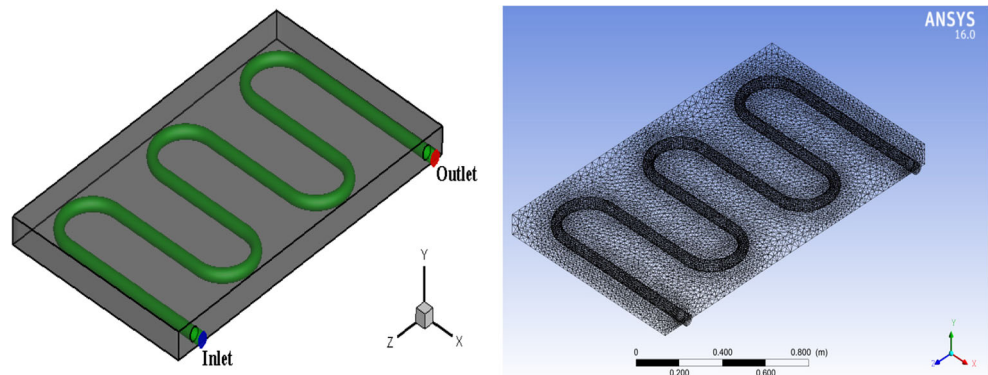


**Table 1** Governing equations used during CFD simulations

Physical Quantity	Equation	Eq. No.
Mass	$\nabla \cdot (\rho \vec{v}) = S_m$	(1)
Momentum	$\nabla \cdot (\rho \vec{v} \vec{v}) = -\nabla p + \nabla \cdot (\vec{\tau}) + \rho + \vec{F}$	(2)
Energy	$\nabla \cdot (\vec{v}(\rho E + p)) = \nabla \cdot (\lambda_{eff} \Delta T - \sum_j h_j J_j + (\vec{\tau}_{eff} \cdot \vec{v})) + S_h$	(3)
Standard $k$ - $\epsilon$ Turbulence Model	$-\rho \overline{u_i u_j} = \mu_t \left( \frac{\partial u_i}{\partial x_j} + \frac{\partial u_j}{\partial x_i} \right) - \frac{2}{3} \rho k \delta_{ij}$	(4)
Radiation Model (P1)	$-\nabla q_r = aG - 4aG\sigma a^4$	(5)

In literature, it is reported that flat plate collectors are best suited for those applications that require low-to-medium temperature heating purposes. Besides that, reported work in the literature suggests that flat plate collectors are constantly progressing for achieving the most appropriate size, which ensures increased thermal efficiency (Bhowmik and Amin 2017; Karki et al. 2019; Khwayyir et al. 2020). The main modifications which are being adopted for enhancing the performance of the collector include modifications in the geometry of the collector, application of the solar selective coatings, and application of nanofluids to increase the heat transfer efficiency of the thermal energy collector (Del Col et al. 2013; Jyothi et al. 2015). Moreover, most of the research is focused on the development stages of the collector. It is an intricate task to measure the accurate performance of the collector due to the huge number of parameters associated with the measurement of the thermal efficiency of the collector (Tagliafico et al. 2014). It is not practically viable to experimentally analyze different collector configurations accurately and economically. Hence, numerical models and different analytical techniques are employed to estimate the performance of the collector at a reasonable accuracy through the use of appropriate approximations and parametric constraints (Tagliafico et al. 2014).

Computational fluid dynamics (CFD) has emerged as a powerful tool for the estimation of transport phenomena. Studies have been carried out on SFPC in various directions to improve understanding of their working mechanism. There have been numerous studies of performance problems with different regional coordinates and tilt angles in the world (Dhimish et al. 2019; Hepbasli and Alsuhaibani 2011; Kambezidis and Psiloglou 2021; Kim et al. 2020; Nsengiyumva et al. 2018). Pakistan is considered a hot region country where there is maximum solar light available throughout the year (Bhutto et al. 2012; Farooq and Kumar 2013; Khan and Pervaiz 2013). However, no literature is available on the affiliation to regional coordinates and the angle of inclination for the performance of SFPC in Pakistan (Unar et al. 2020). Furthermore, there is a need to calculate the optimal tilt angle concerning individual regional coordinates. Moreover, the solar flux at every single coordinate of the earth varies, and hence, it is necessary to test the performance of SFPC at high-temperature regions of the country (Tiko 2019; Wessley and Mathews 2014). Hence, this research primarily focuses on the investigation of performance evaluation concerning different regional coordinates of Pakistan and different tilt angles of SFPC. Moreover, a computational fluid dynamic approach was adopted to

**Fig. 2** Three-dimensional schematic geometry and mesh representation of SFPC

**Table 2** Materials and their thermophysical characteristics

Material used	Density ( $\rho$ ) kg/m <sup>3</sup>	Sp. heat ( $C_p$ ) J/kg K	Thermal conductivity ( $K$ ) W/m-K	Viscosity ( $\mu$ ) kg/m s
Water (liquid)	998.2	4182	0.6	0.001003
Copper (solid)	8978	381	387.6	-
Glass	2489	754	1.75	-
Wood	700	2310	0.173	-

investigate these effects. This research study aimed to develop the 3D CFD model of SFPC to investigate the effects of regional coordinates and tilt angle on SFPC performance. At tilt angles 0°, 15°, 30°, and 45°, the performance of SFPC was measured using regional coordinates.

## Modeling and simulation work

### Overview of methodology

The procedure adopted for CFD simulation work, the geometry of SFPC, meshing, and validation of CFD results are illustrated in Fig. 1. The work is started by an in-depth literature review from which the concerned governing equations and boundary conditions could be extracted. Then, the development of the computational model or meshed geometry phase will start in which the geometry of the selected CFD problem is to be created using standard software and then it is meshed (discretized). After that, the selected governing equations would be numerically solved with the help of a solver and solutions would be collected in the form of contours, surface plots, XY diagrams, path lines, particle trajectories, etc. At this point, the preliminary solution (with the limited set of boundary conditions) is compared with experimental work findings. If the comparison becomes satisfactory, then further simulations would be performed at varying parameters. If the comparison failed and significant differences are observed, then the work needs a repetition from the literature survey where

there may be a change of assumptions, the addition of more neglected governing equations, change of solution strategies, more refinement of the grid, etc.

### CFD model development

The development of the CFD model was carried out in three stages. These steps are called preprocessing, processing, and postprocessing. During preprocessing, advanced software was used to develop the mesh geometry of the selected system. This meshed geometry is technically called the “computational domain.” Therefore, the 3D-geometry of SFPC was made in ANSYS DesignModeler® for this research study as a preprocessing step. After that, usually in the processing steps, transaction CFD codes (Ansys FLUENT®) were used to solve the control equations involved. In this study, the relevant governing equations are tabulated in Table 1. Governing equations were solved through iterations, and convergent cases were obtained.

The given contribution of all the rays crossing into the cell, the radiative transfer equation, was used for describing the radiation phenomena. Furthermore, the discrete ordinate (DO) model was activated and adopted the heat transfer effect between the absorption plate and the protective glass.

The number of spokes selected by the RTE and their directions indicates each radius from the boundary to the path boundary. The general basis for this given method is to quantify the amount of absorption and assume that a given temperature has a constant value within a single control range. The method of calculating the thermal radiation intensity of the element at the node is as follows (Versteeg and Malalasekera 2007):

$$i'_{n+1} = i'_n(1 - \varepsilon(T, x_i)) + i'_b(T)\varepsilon(T, x_i) \tag{1}$$

where  $\varepsilon(T, x_i)$  shows the emissivity,  $i'_b = \sigma \cdot T^4 / \pi$  represents blackbody radiation intensity under controlled

**Table 3** Information on various simulated cases

Name of city	Simulated cases	Working angle	Month
HYD	1 to 12	0°	Jan and Dec
MPK	13 to 24	0°	-
NWS	25 to 36	0°	-
JCA	37 to 48	0°	-
HYD	49 to 60	15°	-
HYD	61 to 72	30°	-
HYD	73 to 84	45°	-
JCA	85 to 96	15°	-
JCA	97 to 108	30°	-
JCA	109 to 120	45°	-

**Table 4** Latitude and longitude of selected cities

Name of city	Short name of city	Latitude (N)	Longitude (E)
Hyderabad	HYD	25.396	68.3578
Mirpurkhas	MPK	25.5065	69.0136
Nawabshah	NWS	26.2447	68.3935
Jacobabad	JCA	28.2823	68.4472

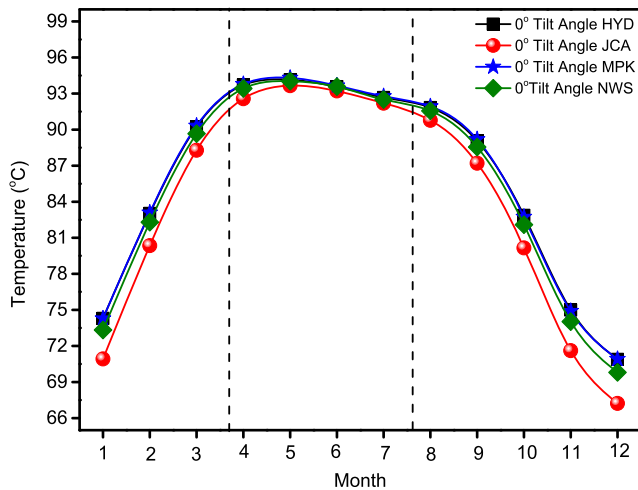


**Fig. 3** Profile of temperature in different cities at a tilt angle of 0°

condition, and  $\sigma$  denotes the Stephan-Boltzmann constant  $5.67 \times 10^{-8} \text{ W/m}^2 \text{ K}^4$ .

### Computational domain

SFPC geometry was developed through the application of ANSYS DesignModler@16. Fig. 2 shows the 3D geometry of the SFPLC having circular tubes. The developed 3D geometry of SFPC with circular tubes is shown in Fig. 2. The circular tube comprises inlet and outlet points for the working fluid. The fluid was inserted from the inlet point of the geometry and flows out of the exit area. The top plate of the SFPC was considered glass. The bottom plate of the SFPC was assumed as a copper absorption plate. The geometry of the cells was tetrahedral. The total number of cells used in the developed computational domain was 538,113, and the minimum orthogonal quality was 0.251. In general, an orthogonal quality greater than 0.2 is considered advantageous for calculations. Besides, a network

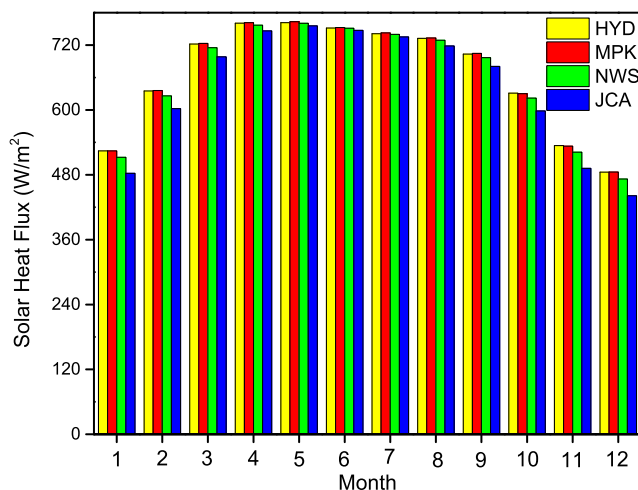


**Fig. 4** On SFPC, average solar heat flux in each month of the year (the range of hours for simulations was from 11: 00 AM to 02:00 PM)

independence test was carried out and it was found that the network gave the best results.

### Assumptions and convergence criteria

It was assumed that the working fluid has a smooth flow. The numerical problem simplifies the heat loss radiation, which is ignored in these cases, and assumed that fluid flow is incompressible under. Flow direction was assumed along the axis of the circular tube. In this investigation, the properties that were taken into consideration include thermophysical properties, thermal conductivity, temperature, and fluid density. Table 2 lists the properties of the wall materials used. The nonslip conditions were put on for wall surfaces. The shell-side conduction method was used to calculate the heat conduction of risers and absorbers. The SIMPLE algorithm between pressure and velocity was used to solve these combinations. The numerical values used for absorber absorptivity and glass transmissivity were 00.95 and 00.91, respectively. The simulation converges when the turbulent kinetic energy residuals contented at  $10^{-3}$ , and radiation at  $10^{-5}$  was attained.

### Operational parameters and boundary conditions

Four cities of Sindh Province were chosen for the performance analysis of SFPC. The selected cities were JCB, MPK, HYD (Hyderabad), and NWS. The performance efficiency of SFPC was inspected throughout the year. The analyses were conducted throughout the year in each month at noon daytime. The inlet water flowrate was set constant at 0.05 kg/s, whereas its temperature was fixed at 27 °C. The tilt angle of SFPC was set as 0°. Furthermore, the analysis was performed by maintaining the tilt angles at 15°, 30°, and 45° in cities HYD and JCB. In Table 3, the geographical coordinates of the selected areas are given, whereas the variations in parameters during simulation are given in Table 4. At tilt angle zero, forty-eight cases were simulated while remaining cases were simulated at different tilt angle variations.

## Results and discussion

### Performance of SFPC at different selected locations

In Fig. 3, the temperature profile of water at 0° tilt angle is shown, whereas in Fig. 4, the average heat flux on SFPC is represented. From Fig. 3 to Fig. 4, it was investigated that water temperature at the outlet of the SFPC increased irrespective of all selected cities and in each month of the year. Furthermore, the performance efficiency of SFPC was observed in April, May, June, and July as compared with the

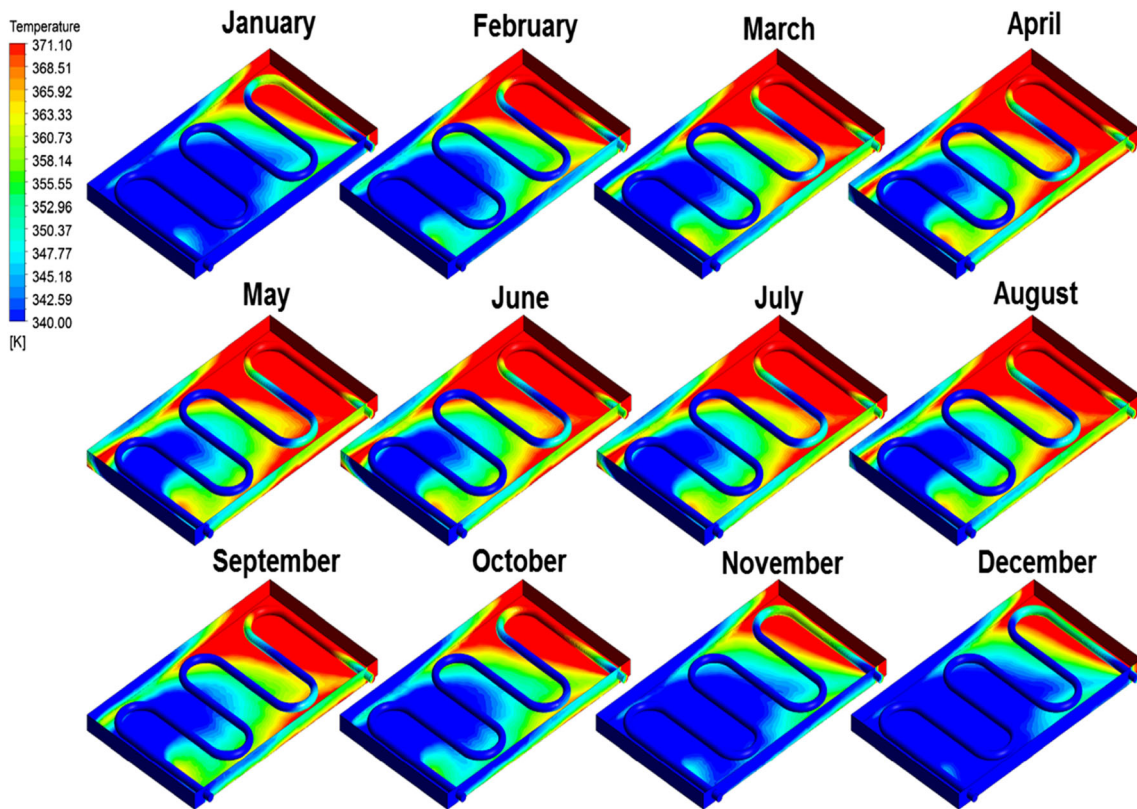


Fig. 5 Local distribution of temperature for HYD at tilt angle 0°

remaining months of the year, while the highest temperature rise in water temperature was found in May and the minimum temperature rise in water temperature was inspected in

December. The highest rise in water temperature was noticed at 94.14 °C in HYD, while the minimum rise in temperature was found at 70.89 °C in HYD. Moreover, the maximum rise

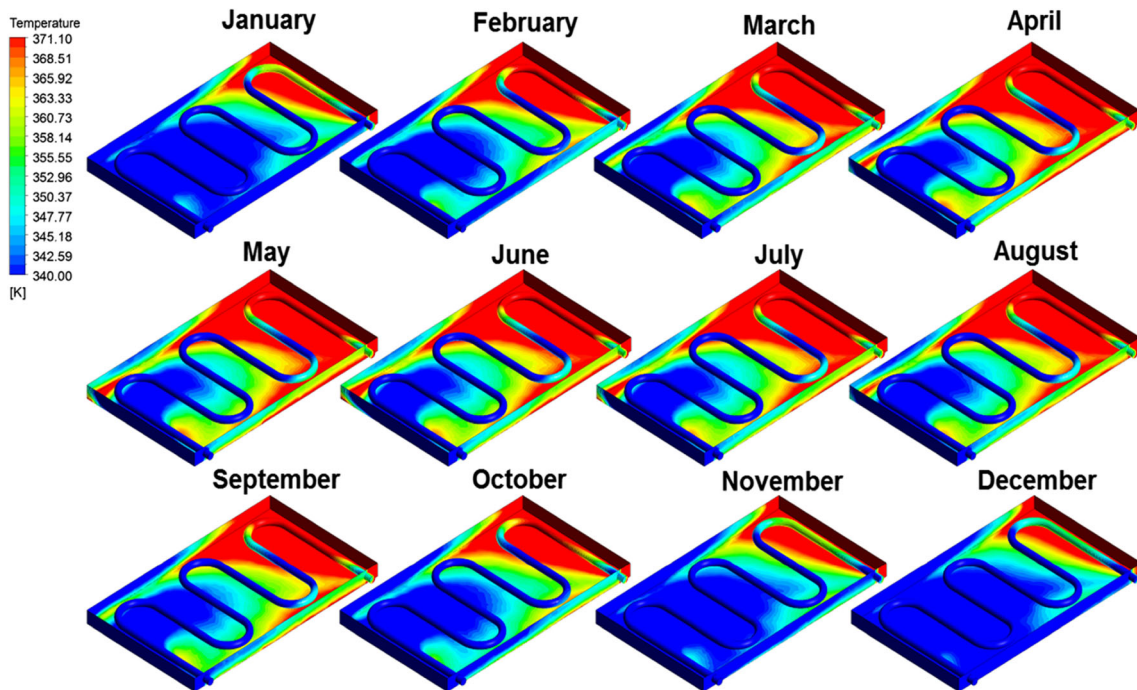
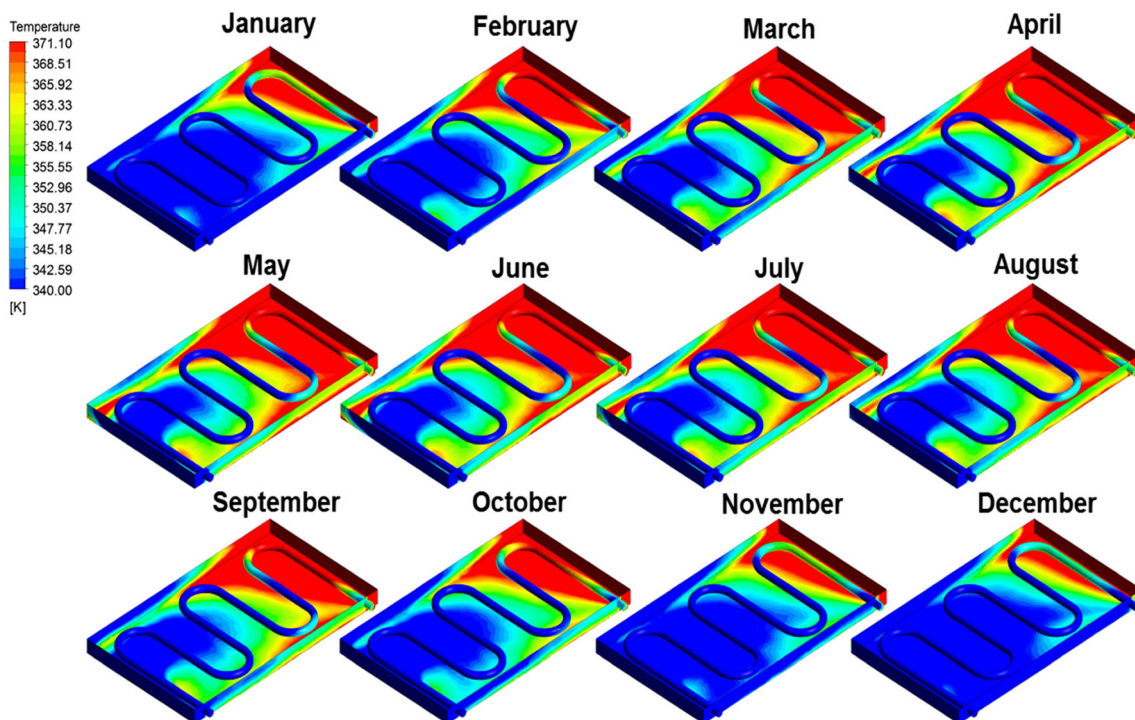


Fig. 6 Local distribution of temperature MPK at tilt angle 0°



**Fig. 7** Local distribution of temperature for NWS at tilt angle  $0^\circ$

in water temperature in the cities MPK, NWS, and JCA was recorded at 94.3, 94.03, and 93.66 °C, respectively, while the minimum rise in working fluid temperature in MPK, NWS, and JCA cities was 70.92, 69.8, and 67.22 °C, respectively. The variation in water temperature rise in all selected cities was due to the variations in solar heat flux in selected locations

as represented in Fig. 4. The solar heat flux on the SFPC collector was maximum in May and minimum in December, while the solar heat flux in December and January was different in JCA as compared to other cities. This change in the solar heat flux was due to the geographical position of JCA.

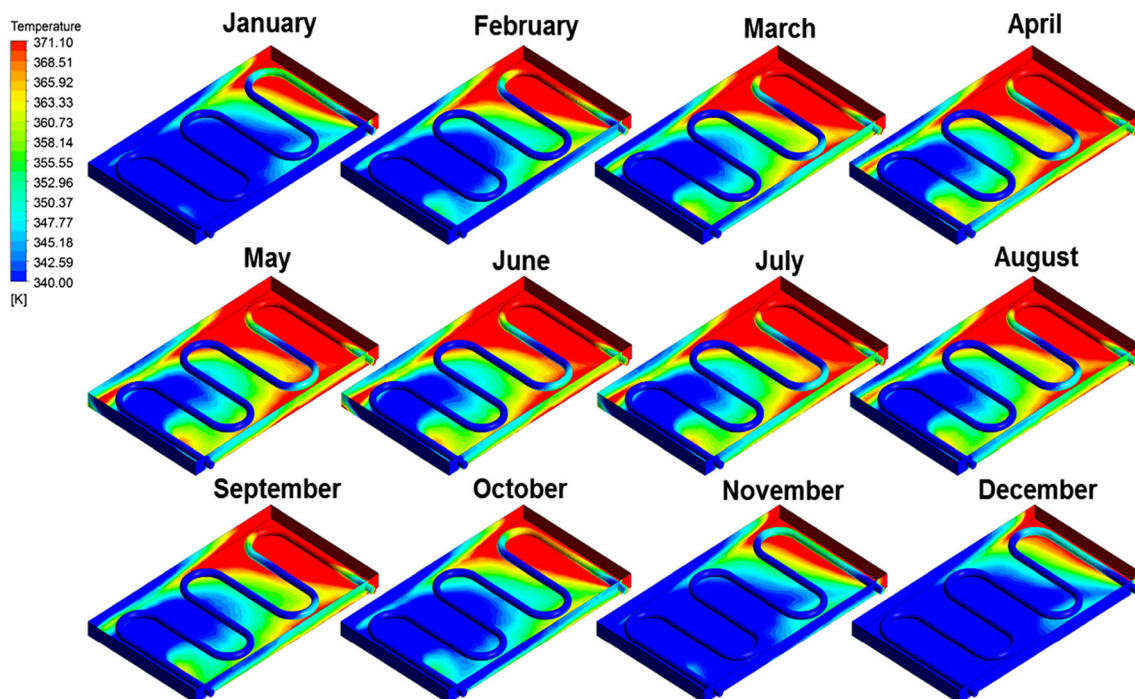


**Fig. 8** Local distribution of temperature for JCA at tilt angle  $0^\circ$

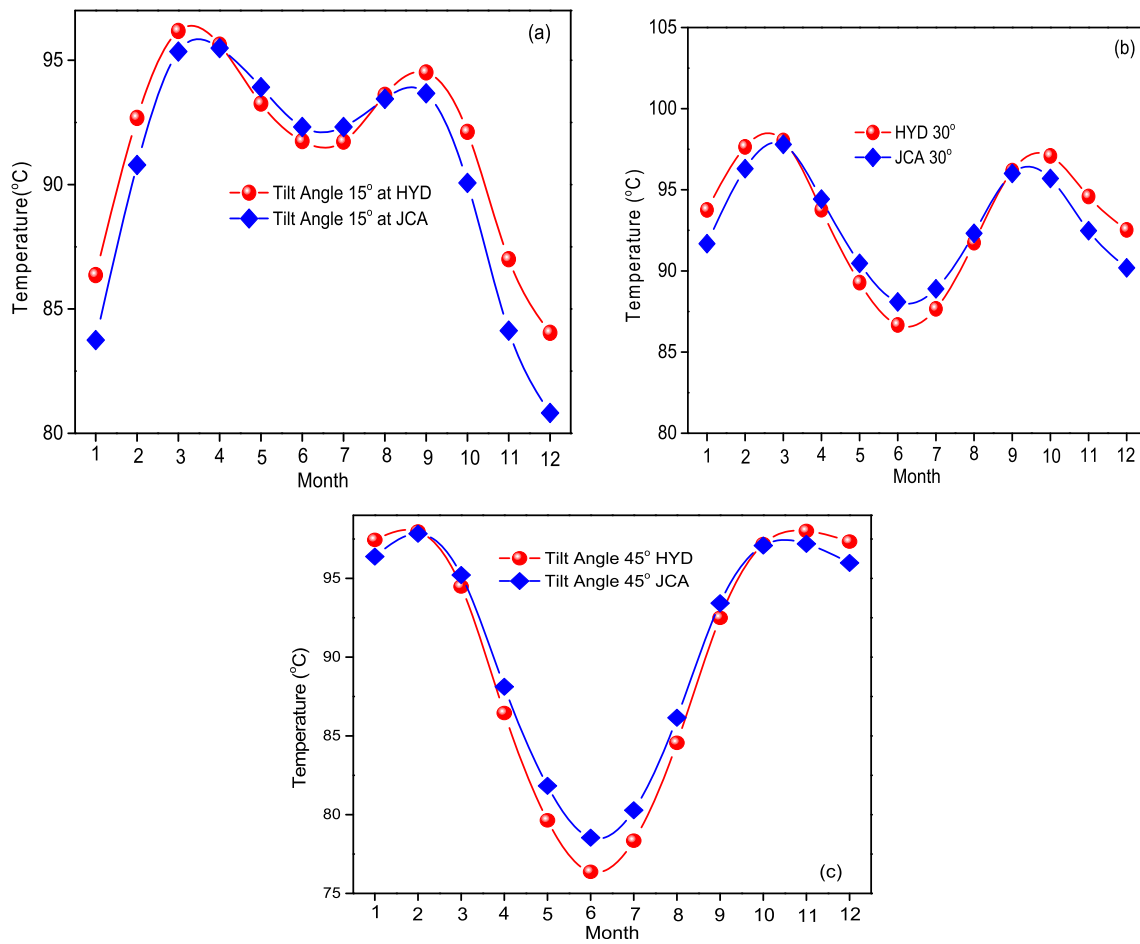


Fig. 9 Regional effect on exit temperature of the water a 15°, b 30°, and c 45°

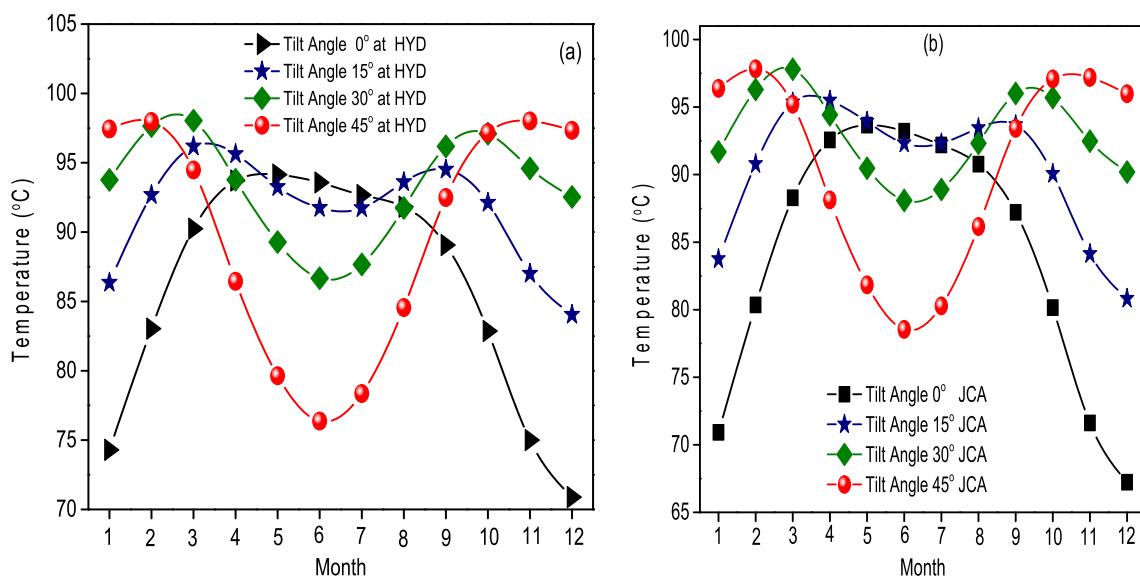
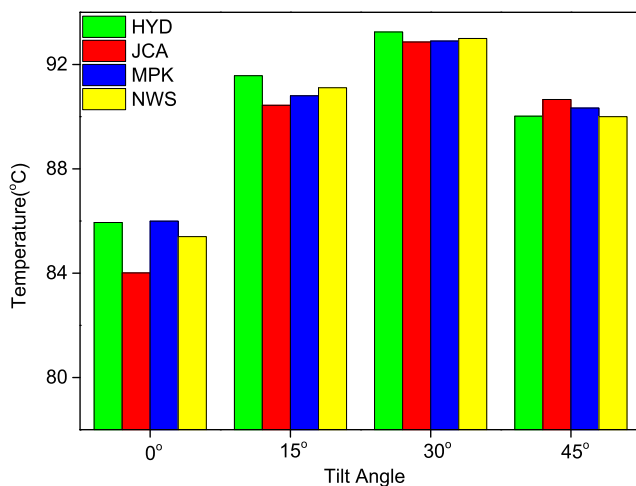


Fig. 10 a, b Exit water temperature at different tilt angles in HYD and JCA





**Fig. 11** All simulated cases and average temperature throughout the year (the range of hours for the simulations was from 11:00 AM to 02:00 PM)

### Local temperature distribution across SFPC

Temperature profiles are assessed to examine the established model qualitatively. The contours of temperature at selected regions are shown colored scale in the area of interest. Temperature contours of the HYD region for each month of the year are shown in Fig. 5 correspondingly, the temperature profile for MPK, NWS, and JCB regions are revealed in Figs. 6, 7, and 8, respectively. From Figs. 5, 6, 7, and 8, effects of the different months on SFPC in terms of shifting of red color in blue color January and December to the summer season (from May to August) were observed. The shadow of the sun in the summer season was maximum as shown in Fig. 5, whereas the contours show that inlet water is represented through blue color at 27 °C temperature. The working fluid temperature increased through the passage along the tube; the heat transferred occurred because of the absorbing plate resulting in enhanced water temperature at the outlet of SFPC.

### Performance analysis of SFPC at angles 0°, 15°, 30°, and 45°

As the temperature contours of SFPC at tilt angle 0° are shown in Figs. 5, 6, 7, and 8, more cases were simulated by keeping the tilt angle in HYD and JCA of SFPC 15°, 30°, and 45°. The results of the simulation study are at different angles 15°, 30°, and 45° as presented in Fig. 9a–c. The rise in water temperature in the summer season was higher as compared with the winter season at a tilt angle of 0°. When tilt angles were raised from 0° to higher, the efficiency of SFPC increased. At higher tilt angles, results collected in the winter season were promising than those in the summer season. Furthermore, the exit water temperature of JCA was slightly less when the comparison was made with the results gathered from HYD in the winter season but higher in

summer. The higher efficiency in the winter season was due to the sun rays were more vertical in winter in HYD as compared to JCA. In JCA, when the tilt angle was maintained at 30°, the absorbing plate efficiency increased in the summer season. The temperature increase in HYD was recorded at a tilt angle of 15° was 96.18 °C in March, whereas in December, temperature rise was noticed at 84.04 °C. In the case of JCA, the maximum and minimum rise in temperature at 15° were measured at 95.49 °C in March and 80.82 °C in December. In HYD, at tilt angle 30°, 98.04 °C was in March and minimum in 86.67 °C in June. These results were found in good agreement with the published results gathered by the author (Kiliç et al. 2018). The maximum exit water temperature in JCB at a tilt angle of 30° was 97.8 °C in March and a minimum of 88.09 °C in June. In HYD at a tilt angle of 45°, the maximum temperature rise was recorded 98.01 °C in November and the minimum was noticing 76.37 °C in June. While in JCA at an angle of 30°, the highest temperature recorded was 97.83 °C in February and a minimum of 78.54 °C in June.

### Comparison of results by varying angles at the same location

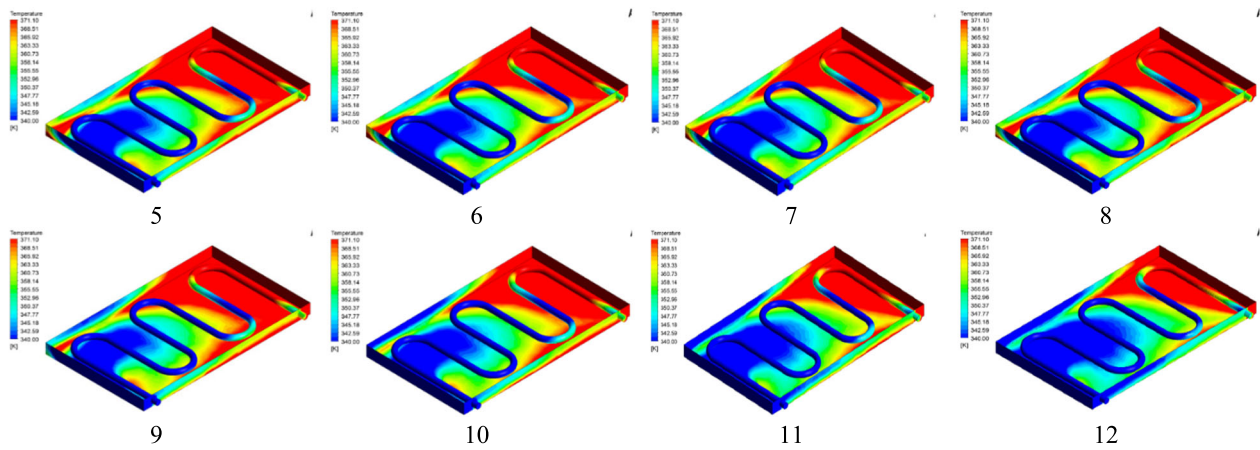
The representation of results at varying geographical coordinates is shown in Fig. 9a–c. Whereas at the same geographical coordinates at varying tilt angles, the results recorded are shown in Fig. 10a, b. Figure 10a shows results in HYD and Fig. 10b represents results of JCB.

It was investigated from the results recorded in Fig. 10a, b, that the overall performance of the SFPC is affected by inappropriate tilt angle. The temperature peaks in summer were higher as compared to those in the winter season.

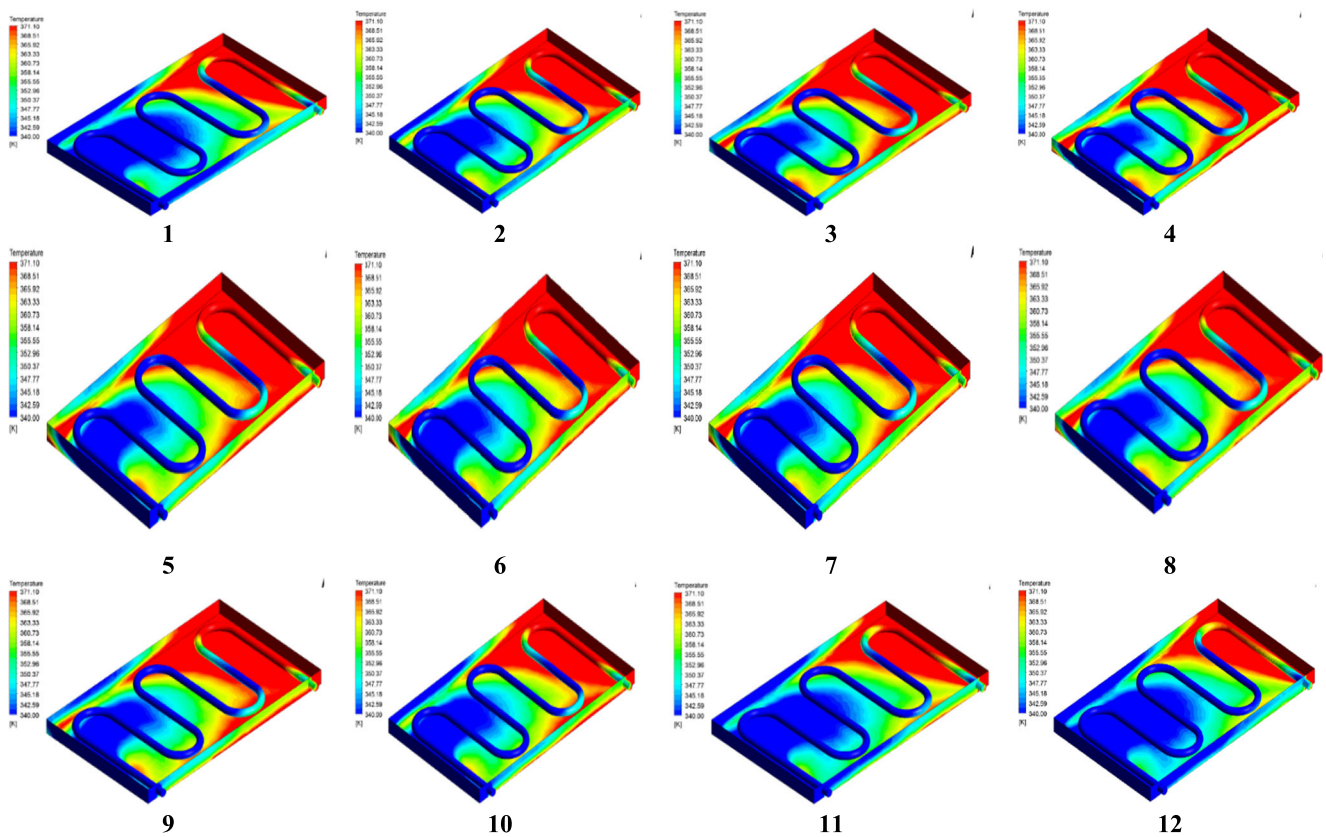
### Variation in angle and its impact on average temperature

From Figs. 5, 6, 7, 8 and 10a–b, results from it were inspected that there was a substantial impression of angle on the efficiency of SFPC but it was hard to determine the appropriate angle for the nominated area. To investigate the appropriateness of the tilt angle, an average temperature was calculated using each scenario. In Fig. 11, the data of average temperature is shown.

The effect of varying angles on the performance of the SFPC in terms of exit water temperature is understandable from Fig. 11. When SFPC was placed at an angle of 0°, the average exit water temperature was recorded from 84 to 86 °C for all nominated locations, while the maximum average temperature at locations HYD and MPK is 86 °C, and in the case of the NWS region, average exit temperature was found at 85.4 °C. Furthermore, the lowest rise in exit water temperature was observed in 84 °C JCA. When the tilt angle was maintained above 0°, the average temperature was increasing with an increase in tilt angle. The highest



(a) Temperature contours in HYD at a 15° tilt angle.



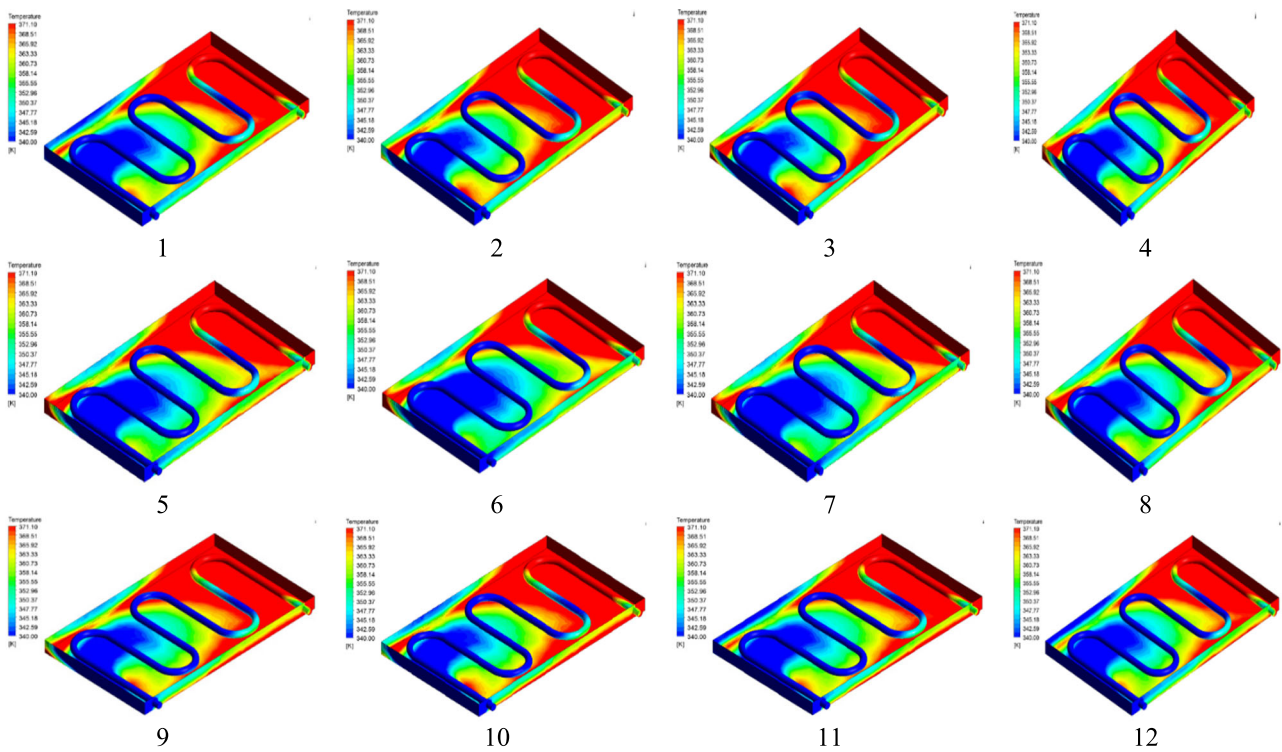
(b) At tilt angle 15°, temperature contours of JCA.

Fig. 12 a Temperature contours in HYD at a 15° tilt angle. b At tilt angle 15°, temperature contours of JCA

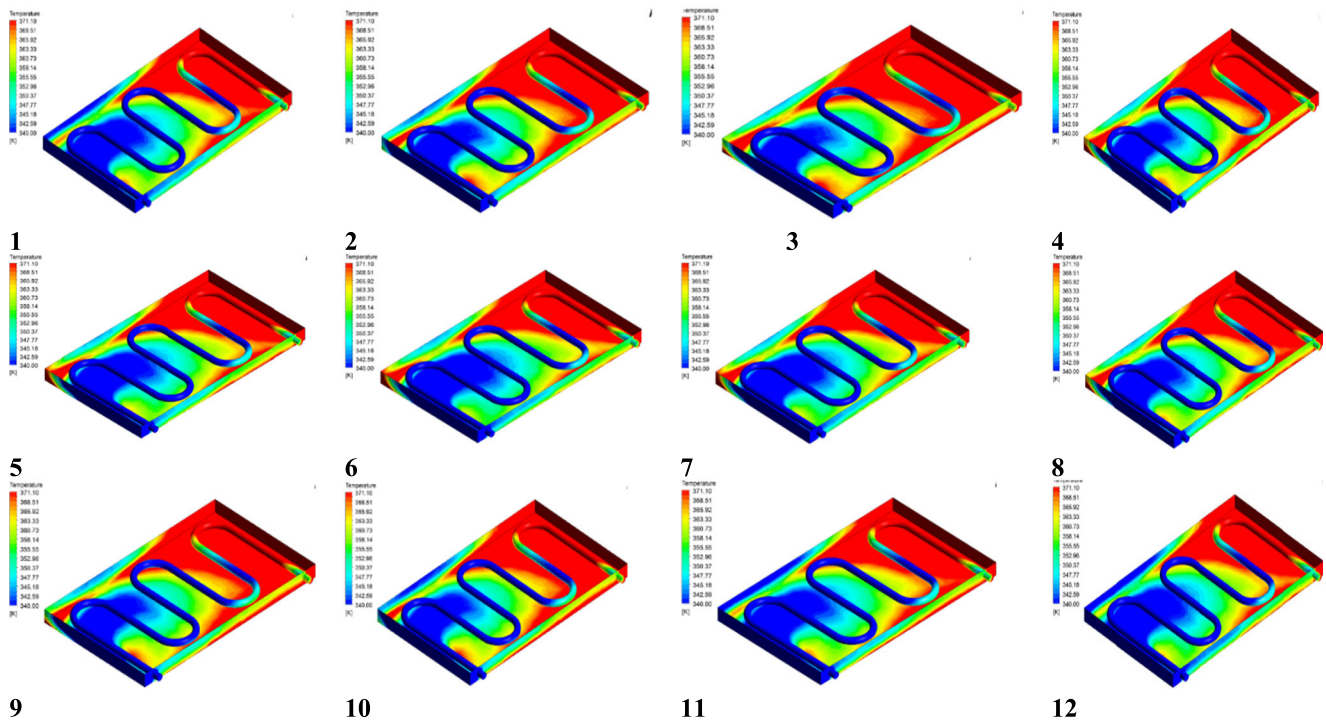
average temperature at the exit of the SFPC was noticed at 92–93 °C at a tilt angle of 30°. Therefore, results suggested that for all selected locations, the maximum efficiency of SFPC was recorded at a tilt angle of 30°. These results were in good agreement with the results gathered by Tiko (2019). The reason for the reduction in average temperature was that beyond the 30° angle, the SFPC was not receiving concentrated solar heat flux owing to its deviation from direct solar irradiation.

### SFPC temperature contours at varying tilt angles

Fig. 12a and b show the contours of the temperature of all the simulated cases having an SFPC tilt angle of 15°. Correspondingly, Figs. 13a, b and 14a, b show contours of the temperature of simulated cases at tilt angles 30° and 45°. The variation in color of contours represented that the temperature profile varied with variations in tilt angle.



(a) Temperature contours in HYD at a 30° tilt angle.



(b) At tilt angle 30°, temperature contours of JCA.

Fig. 13 a Temperature contours in HYD at a 30° tilt angle. b At tilt angle 30°, temperature contours of JCA

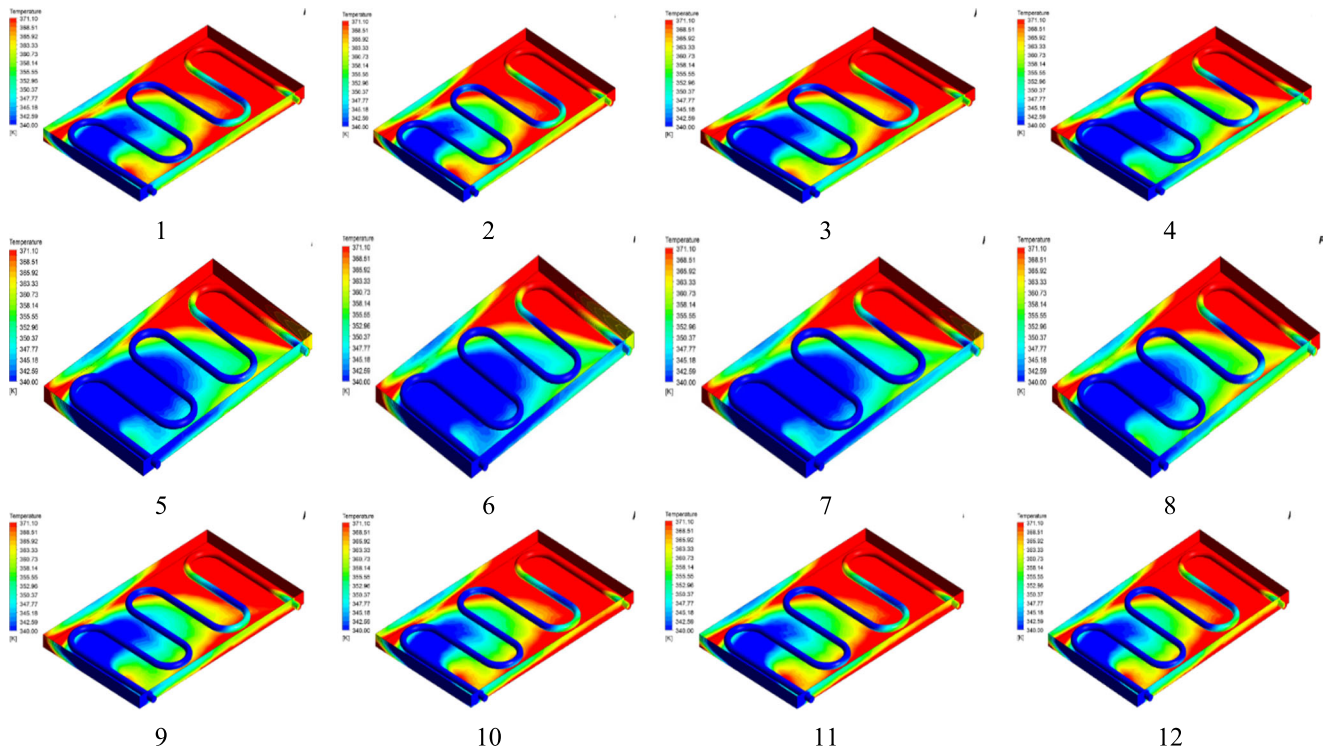
**Conclusions**

Numerical simulation of SFPC was performed through the application Ansys FLUENT software to investigate the

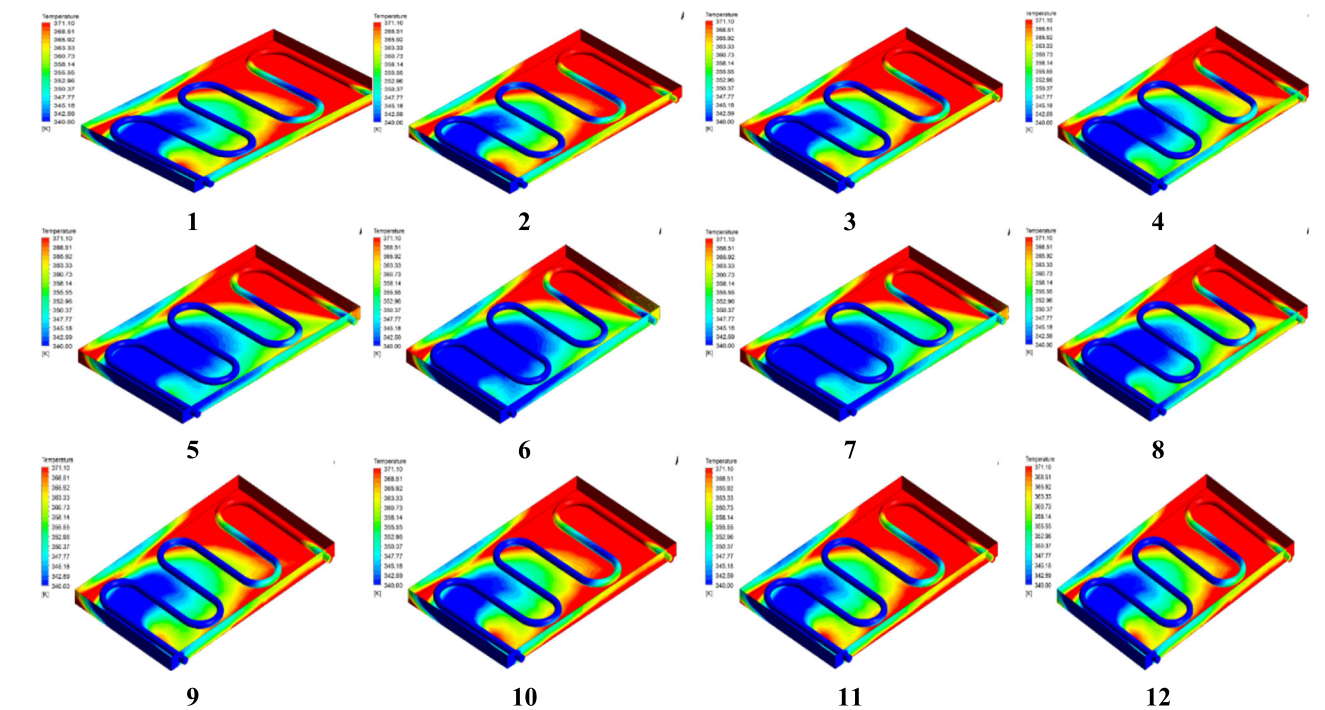
performance of the SFPC at varying regional coordinates and at varying tilt angles in different cities. As working fluid water having an inlet temperature of 27 °C was selected for simulation purposes. To incorporate solar heat flux, solar ray

tracing model was selected using geographical coordinates depending upon the latitude and longitude values. Parallel to ground (at tilt angle 0°) simulations were performed. The

performance of the SFPC was inspected in each month of the year. Furthermore, the tilt angle of the SFPC collector was changed to 15°, 30°, and 45°, respectively. The results



(a) At tilt angle 45°, temperature contours of HYD.



(b) At tilt angle 45°, temperature contours of JCA.

Fig. 14 a At tilt angle 45°, temperature contours of HYD. b At tilt angle 45°, temperature contours of JCA

gathered in four selected cities, using varying coordinates and varying tilt angles, include:

- Parallel to ground, i.e., at tilt angle  $0^\circ$ , initially, the efficiency of SFPC was recorded concerning exit water temperature in each month of the year. After performing simulation at  $0^\circ$  tilt angle, further simulations were run at tilt angles  $15^\circ$ ,  $30^\circ$ , and  $45^\circ$ , respectively.
- The inlet working fluid temperature increased from  $27^\circ\text{C}$  to upper regardless of geographical coordinates.
- Maximum performance of SFPC was observed at tilt angle  $0^\circ$  from April to July.
- In May, the maximum rise in temperature was recorded in all selected districts, while the minimum rise in temperature was recorded in December in all selected regions.
- The maximum temperature rise of  $94.14^\circ\text{C}$  was measured in the Hyderabad district while the minimum temperature was recorded at  $70.89^\circ\text{C}$ .
- Whereas in Mirpurkhas, Nawabshah, and Jacobabad, maximum rise in temperature was noticed at  $94.3^\circ\text{C}$ ,  $94.03^\circ\text{C}$ , and  $93.66^\circ\text{C}$ , respectively.
- Whereas in Mirpurkhas, Nawabshah, and Jacobabad, the minimum rise in water temperature was recorded at  $70.92^\circ\text{C}$ ,  $69.8^\circ\text{C}$ , and  $67.22^\circ\text{C}$ . The maximum temperature was achieved in Mirpurkhas  $94.3^\circ\text{C}$  and minimum in JCA  $67.22^\circ\text{C}$ , respectively.

**Acknowledgements** The author of this research article highly grateful to the Department of Chemical Engineering Mehran University of Engineering and Technology and Dawood University of Engineering and technology for providing a research environment and facilities during this research study.

**Author contribution** Imran Nazir Unar: CFD model development. Ghulamullah Maitlo: data entry and running of CFD cases. Sikandar Ali Abbasi: collection of model results. Masroor Abro: CFD postprocessing of results. Raja Fahad Qureshi and Sheeraz Ahmed Memon: manuscript write-up. Tanveer Hussain and Kashif Hussain Mangi: proofreading and organizing of manuscript.

**Data availability** The data and materials used in this study are available from the corresponding author on reasonable request.

## Declarations

**Ethics approval and consent to participate** Not applicable.

**Consent for publication** Not applicable.

**Competing interests** The authors declare no competing interests.

## References

Akpınar EK, Koçyiğit F (2010) Experimental investigation of thermal performance of solar air heater having different obstacles on

absorber plates. *Int Commun Heat Mass Transfer* 37:416–421. <https://doi.org/10.1016/j.icheatmasstransfer.2009.11.007>

- Akram N et al (2020) A comprehensive review on nanofluid operated solar flat plate collectors. *J Therm Anal Calorim* 139:1309–1343
- Allouhi A et al (2017) Design optimization of a multi-temperature solar thermal heating system for an industrial process. *Appl Energy* 206: 382–392
- Alva G, Lin Y, Fang G (2018) An overview of thermal energy storage systems. *Energy* 144:341–378
- Bhowmik H, Amin R (2017) Efficiency improvement of flat plate solar collector using reflector. *Energy Rep* 3:119–123. <https://doi.org/10.1016/j.egyr.2017.08.002>
- Bhutto AW, Bazmi AA, Zahedi G (2012) Greener energy: issues and challenges for Pakistan—solar energy prospective. *Renew Sust Energ Rev* 16:2762–2780
- Byrne JA, Fernandez-Ibanez PA, Dunlop PS, Alrousan D, Hamilton JW (2011) Photocatalytic enhancement for solar disinfection of water: a review *International Journal of Photoenergy* 2011:111–12
- Chabane F, Moumni N, Benramache S (2014) Experimental study of heat transfer and thermal performance with longitudinal fins of solar air heater. *J Adv Res* 5:183–192
- Choudhury PK, Baruah DC (2017) Solar air heater for residential space heating. *Energy Ecol Environ* 2:387–403. <https://doi.org/10.1007/s40974-017-0077-4>
- Del Col D, Padovan A, Bortolato M, Dai Prè M, Zambolin E (2013) Thermal performance of flat plate solar collectors with sheet-and-tube and roll-bond absorbers. *Energy* 58:258–269
- Dhimish M, Mather P, Holmes V, Sibley M (2019) CDF modelling for the optimum tilt and azimuth angle for PV installations: case study based on 26 different locations in region of the Yorkshire UK IET. *Renew Power Gener* 13:399–408
- Farooq MK, Kumar S (2013) An assessment of renewable energy potential for electricity generation in Pakistan. *Renew Sust Energ Rev* 20: 240–254
- Fathabadi H (2020) Novel low-cost parabolic trough solar collector with TPCT heat pipe and solar tracker: performance and comparing with commercial flat-plate and evacuated tube solar collectors. *Sol Energy* 195:210–222
- France DM, Yu W, Singh D, Kim T (2019) Modular latent heat thermal energy storage systems. Google Patents
- Fudholi A, Sopian K (2019) A review of solar air flat plate collector for drying application. *Renew Sust Energ Rev* 102:333–345
- Hepbasli A, Alsuhaibani Z (2011) A key review on present status and future directions of solar energy studies and applications in Saudi Arabia. *Renew Sust Energ Rev* 15:5021–5050
- Jin H, Lin G, Guo Y, Bai L, Wen D (2020) Nanoparticles enabled pump-free direct absorption solar collectors. *Renew Energy* 145:2337–2344
- Jyothi J, Chaliyawala H, Srinivas G, Nagaraja H, Barshilia HC (2015) Design and fabrication of spectrally selective TiAlC/TiAlCN/TiAlSiCN/TiAlSiCO/TiAlSiO tandem absorber for high-temperature solar thermal power applications. *Sol Energy Mater Sol Cells* 140:209–216
- Kambeizidis HD, Psiloglou BE (2021) Estimation of the optimum energy received by solar energy flat-plate convertors in Greece using typical meteorological years. Part I: South-Oriented Tilt Angles. *Appl Sci* 11:1547
- Karki S, Haapala KR, Fronk BM (2019) Technical and economic feasibility of solar flat-plate collector thermal energy systems for small and medium manufacturers. *Appl Energy* 254:113649. <https://doi.org/10.1016/j.apenergy.2019.113649>
- Khan HA, Pervaiz S (2013) Technological review on solar PV in Pakistan: scope, practices and recommendations for optimized system design. *Renew Sust Energ Rev* 23:147–154

- Khosravi A, Malekan M, Assad ME (2019) Numerical analysis of magnetic field effects on the heat transfer enhancement in ferrofluids for a parabolic trough solar collector. *Renew Energy* 134:54–63
- Khwayyir HS, Baqir AS, Mohammed HQ (2020) Effect of air bubble injection on the thermal performance of a flat plate solar collector. *Therm Sci Eng Progress* 17:100476. <https://doi.org/10.1016/j.tsep.2019.100476>
- Kiliç F, Menlik T, Sözen A (2018) Effect of titanium dioxide/water nanofluid use on thermal performance of the flat plate solar collector. *Sol Energy* 164:101–108
- Kim GY, Han DS, Lee Z (2020) Solar panel tilt angle optimization using machine learning model: a case study of Daegu City, South Korea. *Energies* 13:529
- Kolb A, Winter ERF, Viskanta R (1999) Experimental studies on a solar air collector with metal matrix absorber. *Sol Energy* 65:91–98. [https://doi.org/10.1016/S0038-092X\(98\)00117-0](https://doi.org/10.1016/S0038-092X(98)00117-0)
- Manikandan G, Iniyar S, Goic R (2019) Enhancing the optical and thermal efficiency of a parabolic trough collector—a review. *Appl Energy* 235:1524–1540
- Nahar NM (2003) Year round performance and potential of a natural circulation type of solar water heater in India. *Energy Build* 35: 239–247. [https://doi.org/10.1016/S0378-7788\(02\)00091-9](https://doi.org/10.1016/S0378-7788(02)00091-9)
- Nsengiyumva W, Chen SG, Hu L, Chen X (2018) Recent advancements and challenges in solar tracking systems (STS): a review. *Renew Sust Energy Rev* 81:250–279
- Olczak P, Matuszewska D, Zabagło J (2020) The comparison of solar energy gaining effectiveness between flat plate collectors and evacuated tube collectors with heat pipe: case study. *Energies* 13:1829
- Peng D, Zhang X, Dong H, Lv K (2010) Performance study of a novel solar air collector. *Appl Therm Eng* 30:2594–2601. <https://doi.org/10.1016/j.applthermaleng.2010.07.010>
- Pottler K, Sippel CM, Beck A, Fricke J (1999) Optimized finned absorber geometries for solar air heating collectors. *Sol Energy* 67:35–52. [https://doi.org/10.1016/S0038-092X\(00\)00036-0](https://doi.org/10.1016/S0038-092X(00)00036-0)
- Ramlow B, Nusz B (2010) *Solar water heating—revised & expanded edition: a comprehensive guide to solar water and space heating systems*. New Society Publishers, Gabriola
- Rockenbaugh C, Dean J, Lovullo D, Lisell L, Barker G, Hancock E, Norton P (2016) High performance flat plate solar thermal collector evaluation. National Renewable Energy Lab.(NREL), Golden
- Sarafraz M, Tlili I, Abdul Baseer M, Safaei MR (2019) Potential of solar collectors for clean thermal energy production in smart cities using nanofluids: experimental assessment and efficiency improvement. *Appl Sci* 9:1877
- Syed A, Izquierdo M, Rodriguez P, Maidment G, Missenden J, Lecuona A, Tozer R (2005) A novel experimental investigation of a solar cooling system in Madrid. *Int J Refrig* 28:859–871
- Tagliafico LA, Scarpa F, De Rosa M (2014) Dynamic thermal models and CFD analysis for flat-plate thermal solar collectors—a review. *Renew Sust Energy Rev* 30:526–537. <https://doi.org/10.1016/j.rser.2013.10.023>
- Tiko R (2019) Numerical and experimental investigation of heat transfer enhancement in flat plate collector using nanofluids 2019. ASTU: 1–137
- Tiwari D, Sherwani AF, Asjad M, Arora A (2017) Grey relational analysis coupled with principal component analysis for optimization of the cyclic parameters of a solar-driven organic Rankine cycle Grey Systems: Theory and Application 7:2018–235
- Unar IN, Maitlo G, Ahmed S, Ali SS, Memon AQ, Kandhro GA, Jatoi AS (2020) Performance evaluation of solar flat plate collector using different working fluids through computational fluid dynamics. *SN Appl Sci* 2:1–10
- Versteeg HK, Malalasekera W (2007) *An introduction to computational fluid dynamics: the finite volume method*. Pearson Education, London
- Wessley G, Mathews PK (2014) Experimental analysis of a flat plate solar collector system for small-scale desalination applications. In: *Advanced materials research*. Trans Tech Publ, Stafa-Zurich, pp 800–806
- Zaim EH, Farzan H, Ameri M (2020) Assessment of pipe configurations on heat dynamics and performance of pavement solar collectors: an experimental and numerical study. *Sustain Energy Technol Assess* 37:100635
- Zou B, Dong J, Yao Y, Jiang Y (2016) An experimental investigation on a small-sized parabolic trough solar collector for water heating in cold areas. *Appl Energy* 163:396–407

**Publisher's note** Springer Nature remains neutral with regard to jurisdictional claims in published maps and institutional affiliations.